

This article was downloaded by: [University of Notre Dame]

On: 5 August 2010

Access details: Access Details: [subscription number 917394054]

Publisher Taylor & Francis

Informa Ltd Registered in England and Wales Registered Number: 1072954 Registered office: Mortimer House, 37-41 Mortimer Street, London W1T 3JH, UK



## Geomicrobiology Journal

Publication details, including instructions for authors and subscription information:

<http://www.informaworld.com/smpp/title~content=t713722957>

### Experimental Measurement of Monovalent Cation Adsorption onto *Bacillus subtilis* Cells

Daniel S. Alessi<sup>a</sup>; J. Michael Henderson<sup>a</sup>; Jeremy B. Fein<sup>a</sup>

<sup>a</sup> Department of Civil Engineering and Geological Sciences, University of Notre Dame, Notre Dame, Indiana, USA

Online publication date: 08 June 2010

**To cite this Article** Alessi, Daniel S. , Henderson, J. Michael and Fein, Jeremy B.(2010) 'Experimental Measurement of Monovalent Cation Adsorption onto *Bacillus subtilis* Cells', Geomicrobiology Journal, 27: 5, 464 — 472

**To link to this Article:** DOI: 10.1080/01490450903490813

**URL:** <http://dx.doi.org/10.1080/01490450903490813>

## PLEASE SCROLL DOWN FOR ARTICLE

Full terms and conditions of use: <http://www.informaworld.com/terms-and-conditions-of-access.pdf>

This article may be used for research, teaching and private study purposes. Any substantial or systematic reproduction, re-distribution, re-selling, loan or sub-licensing, systematic supply or distribution in any form to anyone is expressly forbidden.

The publisher does not give any warranty express or implied or make any representation that the contents will be complete or accurate or up to date. The accuracy of any instructions, formulae and drug doses should be independently verified with primary sources. The publisher shall not be liable for any loss, actions, claims, proceedings, demand or costs or damages whatsoever or howsoever caused arising directly or indirectly in connection with or arising out of the use of this material.

# Experimental Measurement of Monovalent Cation Adsorption onto *Bacillus subtilis* Cells

Daniel S. Alessi, J. Michael Henderson, and Jeremy B. Fein

Department of Civil Engineering and Geological Sciences, University of Notre Dame, Notre Dame, Indiana, USA

---

Typically, the effects of ionic strength on metal adsorption to geosorbents are accounted for by models of the surface electric field, assuming a planar surface. However, bacterial cell walls are not two-dimensional surfaces. Furthermore, electric field model parameters for complex systems are difficult to determine and apply. We propose an alternative approach to electric field models of ionic strength effects by explicitly accounting for monovalent cation adsorption onto specific bacterial binding sites. We calculate stability constants for monovalent metal-bacterial surface complexes, and use them to determine the magnitude of correction needed for a previously determined stability constant for a Cd-bacterial surface complex.

---

**Keywords** *Bacillus subtilis*, groundwater, ionic strength, subsurface microbiology, surface complexation

## INTRODUCTION

Surface and groundwaters typically contain a range of metal ions that compete for adsorption sites on surfaces of soil and aquifer components. Although the binding of environmentally important, divalent and trivalent metals onto soil components has been studied (e.g., Beveridge and Murray 1976; Beveridge 1989; Ledin et al. 1997; Yee and Fein 2001; Covelo et al. 2007), the binding behavior of monovalent cations onto bacterial surface functional groups is not known. Monovalent cations represent a major component of the total dissolved ions in many natural waters. Additionally, concentrated solutions of monovalent salts such as NaCl or NaClO<sub>4</sub> typically are used to buffer ionic strength in metal-bacteria adsorption experiments.

---

Received 27 May 2009; accepted 16 November 2009.

This research was supported by the National Science Foundation through an Environmental Molecular Science Institute grant to University of Notre Dame, and by a fellowship from the Arthur J. Schmitt Foundation to D.S.A. J.M.H. was supported by the REU portion of the EMSI grant. We thank Jennifer Szymanowski for assistance with many of the experiments reported here.

Address correspondence to Daniel S. Alessi, Environmental Microbiology Laboratory, Ecole Polytechnique Fédérale de Lausanne, Centre Est 1 543, CH-1015 Lausanne, Switzerland. E-mail: daniel.alessi@epfl.ch

The adsorption of monovalent cations onto mineral and bacterial surfaces has been accounted for indirectly through construction of electric double or triple layer models, which ascribe the association of the cations with the surface to electrostatic interactions with the surface electric field (Stumm et al. 1970; Davis et al. 1978). Implicit in electrostatic surface complexation models of experimental adsorption data is the assumption that monovalent cations do not compete with higher-charged metals for adsorption onto specific bacterial surface functional groups.

Typically, the adsorption of multivalent cations to minerals and bacteria decreases with increasing ionic strength (e.g., Daughney and Fein 1998; Gu and Evans 2008). Electrostatic multi-layer models ascribe these ionic strength effects to the contraction of the surface electric field of the sorbent due to non-specific outer-sphere electrostatic attraction of monovalent counterions to the electric field of the sorbent (e.g., Davis and Kent 1990; Koretsky 2000). However, electrostatic models require the optimization of a number of parameters from experimental data such as surface electric field capacitance values. Direct model-independent determination of these parameters is impossible, and application of these models to complex real systems is problematic (Davis et al. 1998).

An alternative approach to accounting for ionic strength effects on multi-valent cation adsorption is to ascribe the adsorption behavior to direct competition between the electrolyte monovalent cations and the less abundant multivalent cations for specific surface sites. In this approach, associations between metal cations and cell wall functional groups are treated as aqueous complexation reactions, analogous to the Bjerrum ion-ion interaction approach in aqueous solutions (Bjerrum 1926). This approach obviates the need for determining electrostatic modeling parameters by instead including electrostatic effects in the apparent metal-surface equilibrium constants (Davis and Kent 1990). Equilibrium constants determined using this approach have the advantage of being independent of ionic strength and pH. Although the binding between surface functional groups and monovalent cations is likely to be weak, the concentration of the background electrolyte in metal adsorption experiments is often several orders of magnitude greater than that of the metal of interest. Thus, it is possible that monovalent metals

significantly reduce the adsorption of higher charged metals via specific adsorption onto sites at the bacterial surface.

In this paper, we report the results of experiments conducted to determine the extent of adsorption of three monovalent cations,  $\text{Li}^+$ ,  $\text{Rb}^+$ , and  $\text{Na}^+$ , to the Gram-positive soil bacterial species *Bacillus subtilis* as a function of ionic strength and pH. Adsorption data are modeled using a non-electrostatic surface complexation model (NEM) approach, and discrete metal-bacteria binding constants are determined for each monovalent cation. These constants are then used to determine the competitive effect of monovalent cations on the adsorption of Cd at bacterial surface sites.

## METHODS

### Bacteria Growth and Preparation

The Gram-positive soil bacterium *Bacillus subtilis* was initially cultured on agar slants made of 0.5% yeast extract and trypticase soy agar. Cells from the slant were transferred to 3 ml of growth medium consisting of trypticase soy broth (TSB) and 0.5% yeast extract and allowed to grow for 24 hours at 32°C. After the growth period, these bacteria were transferred to 2 l of identical broth and allowed to grow for another 24 hours at 32°C, reaching stationary phase. Bacteria were harvested by centrifuging the broth at 9,000 g for 10 minutes to pellet the bacteria.

After decanting the broth, the bacteria were washed four times in  $\text{NaClO}_4$  electrolyte solutions of the same ionic strength as the target ionic strength for an individual adsorption experiment, between  $10^{-3}$  and  $10^{-1}$  M. After each wash, the bacteria were centrifuged at 8100 g for 5 minutes to pellet the bacteria and the electrolyte was discarded. The cells were then resuspended in fresh electrolyte using a Vortex and stir rod. The bacteria were transferred to a weighed centrifuge tube after the final wash, and centrifuged two times for 30 minutes at 8100 g, decanting the remaining supernatant each time. The weight of the resulting wet bacterial pellet has been determined to be 8 times the dry weight (Borrok et al. 2005). The growth and washing procedure renders the bacteria alive, but metabolically inactive (Borrok et al. 2007).

### $\text{Li}^+$ and $\text{Rb}^+$ Adsorption Experiments

Batch metal-bacteria adsorption experiments were performed with the monovalent cations  $\text{Li}^+$  and  $\text{Rb}^+$  (separately) in the presence of a  $\text{NaClO}_4$  electrolyte, as a function of  $\text{NaClO}_4$  concentration and pH. A perchlorate electrolyte solution was chosen because this anion does not complex strongly with metal cations. Because Na and K are present in biological cells and leach into solution to some extent, it is impossible to conduct adsorption experiments with these elements due to mass balance difficulties. Instead, we conducted  $\text{Li}^+$  and  $\text{Rb}^+$  adsorption measurements because these elements are not present appreciably in cells, and therefore rigorous constraints on their mass balances could be imposed on the experimental systems.

To verify that  $\text{Li}^+$  or  $\text{Rb}^+$  did not enter into electrolyte solutions from within the cells, control experiments were performed by suspending 20 g  $\text{l}^{-1}$  wet mass *B. subtilis* cells in  $10^{-1}$ ,  $10^{-2}$ , and  $10^{-3}$  molal  $\text{NaClO}_4$  electrolyte solutions. Each ionic strength bacterial suspension was separated into a set of test tubes, and the pH of each tube was adjusted using small volumes of HCl or NaOH to a value between 2 and 10. The tubes were placed on a rotary shaker to equilibrate for 2 h, after which the steady-state pH of each system was measured.

The systems were then centrifuged at 8100 g for 10 min to separate the bacteria from the solution, and the resulting supernatants filtered through 0.45  $\mu\text{m}$  nylon membranes and acidified with 25  $\mu\text{L}$  of 2.0 M HCl per 10 ml of solution. Metal concentrations in all solutions were immediately analyzed using Inductively Coupled Plasma – Optical Emission Spectrometry (ICP-OES). In all control experiments, the measured concentrations of  $\text{Li}^+$  and  $\text{Rb}^+$  were below the detection limits of the ICP-OES, determined to be 0.05 ppm for  $\text{Li}^+$  and 0.1 ppm for  $\text{Rb}^+$ .

Isotherm  $\text{Li}^+$  and  $\text{Rb}^+$  adsorption experiments were performed as a function of ionic strength at a range of fixed pH values between pH 3 and 9. Each experiment was initiated by suspending 20 g  $\text{l}^{-1}$  wet mass *B. subtilis* in a  $\text{NaClO}_4$  electrolyte solution with a concentration between  $10^{-1}$  and  $10^{-3}$  M. The pH of each suspension was adjusted as needed with small volumes of NaOH or HCl, and the systems were allowed to equilibrate on a rotary shaker for 2 h. This process of pH adjustment was repeated until each system was within  $\pm 0.1$  units of the target pH. The amount of acid or base added was recorded in order to calculate the final experimental ionic strength value.

After each suspension reached steady-state pH conditions, 10 ml aliquots of the bacterial suspension were removed from each system, placed into polypropylene test tubes, spiked to a final concentration of  $2.34 \times 10^{-5}$  M  $\text{Li}^+$  or  $\text{Rb}^+$  using 1000 mg  $\text{l}^{-1}$  Li or Rb stock solutions prepared from  $\text{LiClO}_4$  or  $\text{RbClO}_4$  salts, and allowed to react for another 2 h. The preparation of these  $\text{LiClO}_4$  and  $\text{RbClO}_4$  stock solutions and all additions of the solutions to experiments were performed gravimetrically. After reaching steady-state, the pH of experimental systems with  $\text{Li}^+$  and  $\text{Rb}^+$  were measured. The final pH levels for the  $\text{Li}^+$  experiments were  $2.99 \pm 0.03$ ,  $4.99 \pm 0.03$ ,  $6.95 \pm 0.07$ , and  $9.19 \pm 0.09$ , and for the  $\text{Rb}^+$  experiments,  $2.98 \pm 0.03$ ,  $5.18 \pm 0.10$ ,  $6.98 \pm 0.04$ , and  $9.02 \pm 0.04$ . Henceforth, for convenience we refer to these experiments as pH 3, 5, 7, and 9, respectively.

The test tubes were centrifuged, filtered, and acidified in the same manner as the control experiments (described above), and metal concentrations in the solutions were immediately analyzed using ICP-OES. We found that the signal strength of the ICP-OES varied strongly with solution ionic strength and composition (data not shown). To control for this effect, we centrifuged and filtered the extra Li- and Rb-free bacterial suspension that was not used in each  $\text{Li}^+$  and  $\text{Rb}^+$  adsorption experiment, and made Li or Rb calibration standards for

ICP-OES analysis using the resulting supernatants. In this way, each experimental system had its own set of calibration standards made in a background matrix that was identical to that of the experimental samples.

Analytical uncertainties associated with the ICP-OES analysis, as determined by repeat analyses of calibration standards, were less than  $\pm 3\%$  in all cases. The amount of metal adsorbed in each experimental system was determined by subtracting the measured metal concentration remaining in solution from the initial known metal concentration in each experiment.

### Cd Adsorption Experiments

Batch Cd metal adsorption experiments were performed between pH 2.0 and 5.5 in the presence of Li-, Na-, and  $\text{KClO}_4$  electrolytes to determine if the type of monovalent cation in the buffering electrolyte affected Cd adsorption behavior. Experiments were initiated by suspending  $20 \text{ g l}^{-1}$  washed *B. subtilis* cells in a  $0.1 \text{ M}$  Li-, Na-, or  $\text{KClO}_4$  solution containing  $8.90 \times 10^{-5} \text{ M}$  Cd from a  $1000 \text{ mg l}^{-1}$  Cd stock solution. The Cd stock solution was prepared from a  $\text{Cd}(\text{ClO}_4)_2$  salt. The experimental pH adjustments, equilibration time, centrifugation, filtering, and acidification for each system was identical to the procedures used for  $\text{Li}^+$  and  $\text{Rb}^+$  batch adsorption experiments described previously.

Concentrations of Cd remaining in the filtered supernatants were analyzed using ICP-OES. Cd standards were prepared gravimetrically from a  $1000 \text{ mg l}^{-1}$  Cd stock solution made from a  $\text{Cd}(\text{NO}_3)_2$  salt, diluted to desired concentrations using the same perchlorate salt matrix as the experimental systems being analyzed. The Cd signal strength reported by the ICP-OES did not vary significantly with solution ionic strength, and uncertainties were within  $\pm 3\%$  for these experiments.

### RESULTS

The measured extents of  $\text{Li}^+$  and  $\text{Rb}^+$  adsorption onto *B. subtilis* are shown as a function of ionic strength at various pH values in Figures 1 and 2, respectively. The addition of NaOH to achieve the pH 9 conditions, or HCl to achieve pH 3 and 5, substantially increases the ionic strength of the background electrolyte in the experiments that had an initial ionic strength of  $10^{-3} \text{ M}$ . For this reason, each experiment is plotted using the actual ionic strength of the experiment, which is the sum of the ionic strength contribution from the  $\text{NaClO}_4$  electrolyte and that from the acid or base additions.

In both the  $\text{Li}^+$  and  $\text{Rb}^+$  experiments, no significant adsorption is observed at any ionic strength in experiments conducted at pH 3, whereas significant adsorption is observed in the pH 5, 7, and 9 experiments. The pH 5, 7, and 9 experimental results indicate that the extent of Li and Rb adsorption increases significantly with decreasing ionic strength of the experimental electrolyte. As a function of pH, the amount of metal adsorbed to the bacteria in the pH 5, 7, and 9 experiments does not change significantly at any ionic strength level. This suggests that at pH 5

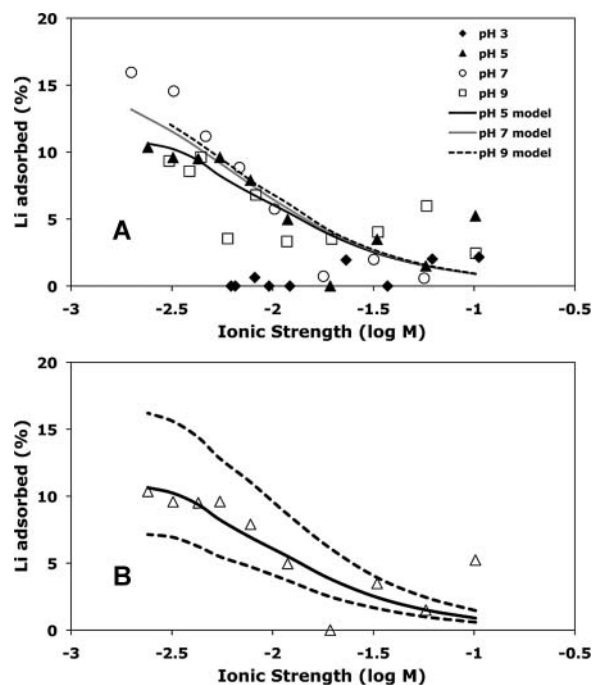


FIG. 1. (A) Lithium adsorption to *B. subtilis* as a function of ionic strength and pH. Initial experimental conditions were  $20 \text{ g l}^{-1}$  *B. subtilis* cells and  $2.34 \times 10^{-5} \text{ M}$  Li. The pH 5 model curve represents the best-fit model that accounts for Li adsorption onto Site 2 only. Curves for the pH 7 and pH 9 models show the extent of adsorption that would be predicted using the  $K_{Na}$  and  $K_{Li}$  values determined from modeling the pH 5 data, and assuming no additional adsorption of Li onto Sites 3 or 4. (B) Best-fit model for Li adsorption to Site 2 of *B. subtilis* at pH 5 (solid curve). Dashed curves are models resulting from a  $\pm 0.2$  variation in the best-fitting log stability constant value of  $K_{Li}$ .

and above, Li and Rb adsorption behavior is more dependent on ionic strength than pH under our experimental conditions.

Figure 3 shows the results of the experiments of Cd adsorption onto *B. subtilis* cells. Cd adsorption increases as a function of increasing pH from approximately 10% at pH 2 to nearly 80% at pH 5.5. The extent of adsorption does not vary significantly as a function of the type of monovalent salt used to buffer the ionic strength of the experimental system, suggesting that the three monovalent cations studied here compete with Cd for adsorption to bacterial surface functional groups to a similar degree.

In general, the extent of adsorption of the monovalent cations studied here was much less than that observed for divalent cations under similar experimental conditions. In the experiments conducted at an ionic strength of  $10^{-1} \text{ M}$ , adsorption of Li and Rb was approximately 5% or less under the pH conditions studied; in experiments with an ionic strength of  $10^{-2.5} \text{ M}$ , the maximum extent of Li and Rb adsorption that was observed under any of the pH conditions was 10–15%. To compare, the Cd adsorption experiments reported here were conducted at an ionic strength of  $0.1 \text{ M}$ , using the same bacterial concentration as we used in the Li and Rb experiments. Although the Cd molality in these experiments is nearly four times that of Li or Rb

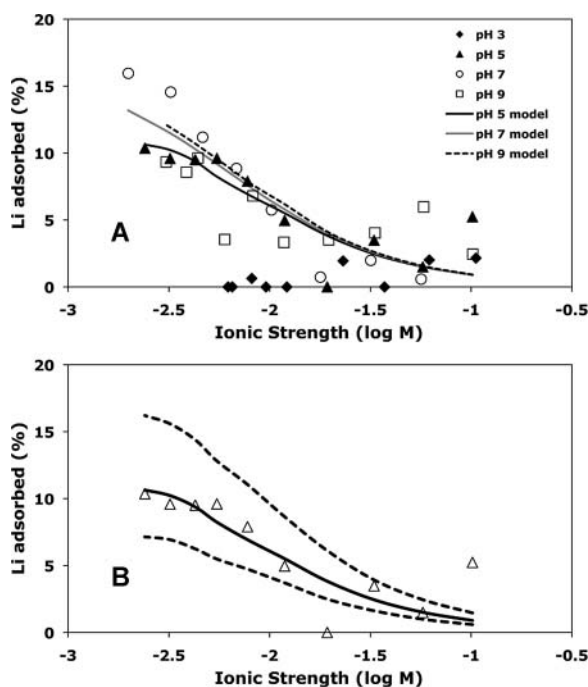


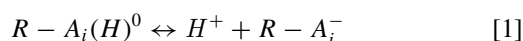
FIG. 2. (A) Rubidium adsorption to *B. subtilis* as a function of ionic strength and pH. Initial experimental conditions were  $20 \text{ g l}^{-1}$  *B. subtilis* cells and  $2.34 \times 10^{-5} \text{ M}$  Rb. The pH 5 model curve represents the best-fit model that accounts for Rb adsorption onto Site 2 only. Curves for the pH 7 and pH 9 models show the extent of adsorption that would be predicted using the  $K_{Na}$  and  $K_{Rb}$  values determined from modeling the pH 5 data, and assuming no additional adsorption of Rb onto Sites 3 or 4. (B) Best-fit model for Rb adsorption to Site 2 of *B. subtilis* at pH 5 (solid curve). Dashed curves are models resulting from a  $\pm 0.2$  variation in the best-fitting log stability constant value of  $K_{Rb}$ .

in their adsorption experiments, approximately 75% of the Cd in solution adsorbed onto cell walls at pH 5 (Fig. 3A), compared to less than 5% adsorption for the Li and Rb.

## DISCUSSION

### Thermodynamic Modeling

The objective of the thermodynamic modeling of the experimental data was to determine if a stability constant for the monovalent-bacterial surface complex could account for the adsorption behavior as a function of  $\text{NaClO}_4$  content for each cation studied. We use a nonelectrostatic surface complexation model to describe proton and metal adsorption onto the cell wall functional groups of *B. subtilis*. A system of mass action equations is used to calculate the distribution of protons and metal cations between the bacterial cell wall functional groups and the solution. In this approach, the proton deficit on the cell wall, relative to the zero proton condition of a fully protonated cell wall (Fein et al. 2005), is ascribed to the deprotonation behavior of cell wall-associated organic acid functional groups:



where  $A_i$  represents a distinct organic acid functional group type, and  $R$  represents the bacterial cell wall macromolecule to which the functional group  $A_i$  is attached. The mass action equation for the deprotonation reaction is:

$$K_a = \frac{[R - A_i^-] a_{H^+}}{[R - A_i(H)^0]} \quad [2]$$

where  $K_a$  is the equilibrium constant, or acidity constant, for Reaction (1), the brackets represent molar concentrations of the bacterial surface species, and is the activity of protons in the bulk solution. We use a four-site ( $i = 1 - 4$ ) nonelectrostatic model (NEM), described by Fein et al. (2005). We refer to these sites as Sites 1 – 4, respectively, and Table 1 lists the pKa and concentration of each cell wall functional group.

Bulk adsorption observations can not be used to distinguish between cation binding to specific bacterial surface sites and nonspecific cation binding that results from electrostatic attraction by a surface electric field. Our objective is to model this interaction as binding to specific sites, and therefore as a competition reaction. Experimental measurements of the extent of adsorption as a function of pH in single-metal systems can be used to constrain which sites are involved in the adsorption reactions and to determine the stability constants for the important bacterial surface complexes (e.g., Fein et al. 1997; Cox et al. 1999; Haas et al. 2001; Ngwenya et al. 2003). However, there are two competing types of monovalent cations present in each of our experimental systems:  $\text{Li}^+$  or  $\text{Rb}^+$  as the adsorbing metal of interest, and  $\text{Na}^+$  from the  $\text{NaClO}_4$  ionic strength buffer. We explicitly account for competition by including metal binding reactions for both cations that are present in each system in our

TABLE 1

Model fits of potentiometric titration data for *Bacillus subtilis* cells

	NEM <sup>1</sup>	NEM with $\text{Na}^{+2}$	DLM <sup>3</sup>
pKa <sub>1</sub>	3.1	2.5	1.7
[R-L <sub>1</sub> ] <sup>4</sup>	78	79	210
pKa <sub>2</sub>	4.7	4.0	4.2
[R-L <sub>2</sub> ] <sup>4</sup>	109	111	54
pKa <sub>3</sub>	7.2	6.5	6.3
[R-L <sub>3</sub> ] <sup>4</sup>	55	55	98
pKa <sub>4</sub>	9.4	8.6	
[R-L <sub>4</sub> ] <sup>4</sup>	89	91	

Titration data from Fein et al. (2005).

1 Nonelectrostatic model.

2 Model that includes  $\text{Na}^+$  binding onto each bacterial surface functional group, with a  $\log K_{Na} = 1.8$ .

3 Diffuse layer model.

4 Site concentrations in  $\mu\text{mol g}^{-1}$ .

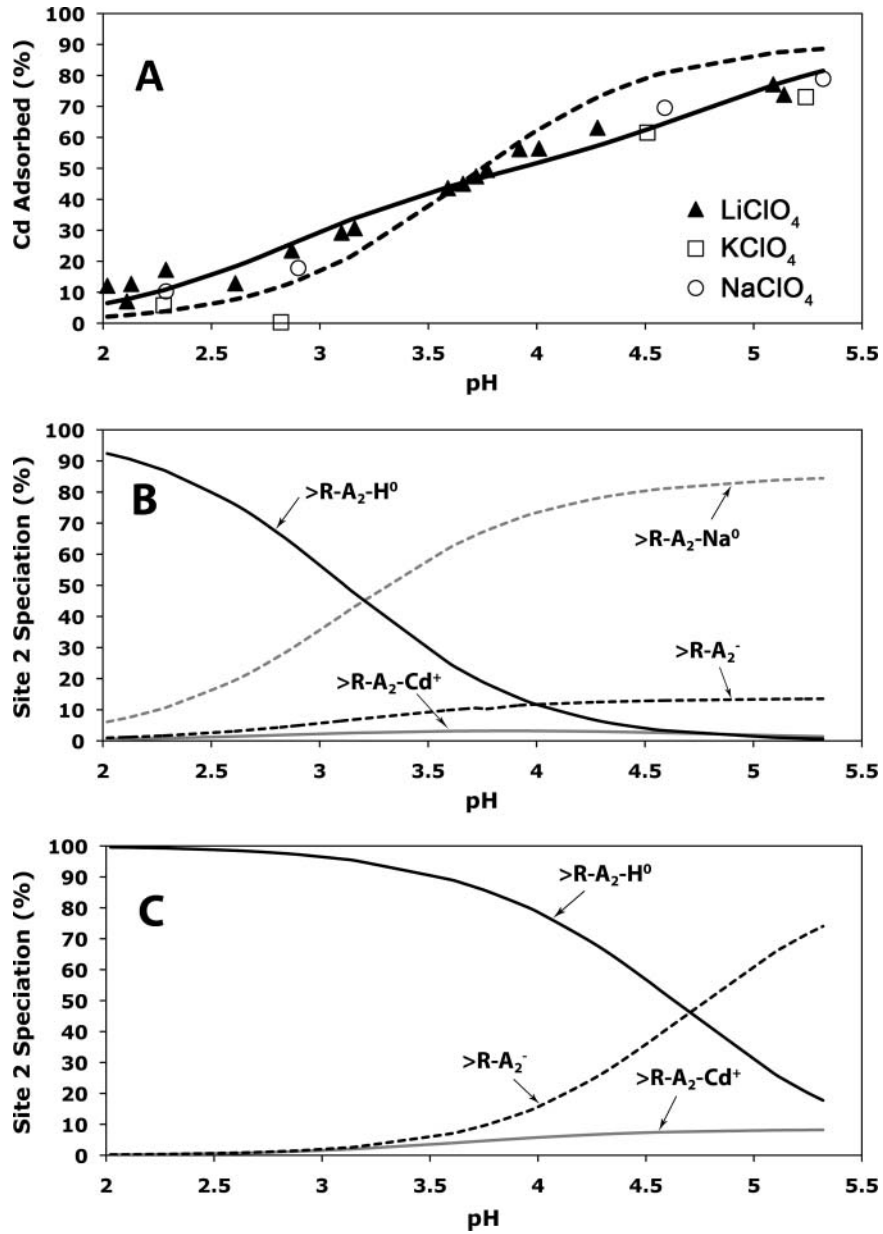
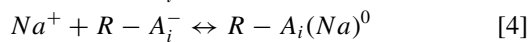
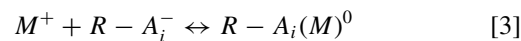


FIG. 3. (A) Cd adsorption to *B. subtilis* cells in Na-, K-, and Li-perchlorate electrolytes. Initial experimental conditions were 10 g l<sup>-1</sup> *B. subtilis* cells and 8.90 × 10<sup>-5</sup> M Cd in a 0.1 M perchlorate solution. Curves indicate the best-fit models for Cd adsorption onto bacterial Site 2 with (solid curve) and without (dashed curve) inclusion of the Na-Site 2 complexation reaction in the model. The speciation of Site 2, with and without Na-Site 2 complexation, is depicted in (B) and (C), respectively.

models according to:



where  $M^+$  represents the monovalent metal of interest (Li<sup>+</sup> or Rb<sup>+</sup>) in reaction (3). The equilibrium constants ( $K_{eq}$ ) for

complexation reactions (3) and (4) are defined by:

$$K_M = \frac{[R - A_i(M)^0]}{[R - A_i^-] a_{M^+}} \quad [5]$$

$$K_{Na} = \frac{[R - A_i(Na)^0]}{[R - A_i^-] a_{Na^+}} \quad [6]$$

respectively, where  $[R - A_i^-]$  represents the concentration of deprotonated cell wall functional group  $A_i$ ,  $[R - A_i(M)^0]$  represents the concentration cell wall functional group  $A_i$  that is complexed with metal  $M$ , and  $a_{M^+}$  is the activity of the monovalent metal of interest in solution after equilibrium is attained.

Equations (2), (5), and (6) can be used, together with pH measurements, measurements of the extent of Li or Rb and Na adsorption, and mass balance constraints on Na and Li or Rb concentrations, to determine the unknown values of  $K_M$  and  $K_{Na}$ . However, because the extent of Na that adsorbs in each experiment cannot be measured directly, it is not possible to solve for  $K_{Na}$  directly. We can use multiple measurements of Li or Rb adsorption, in experiments conducted with varying total Na concentrations, to constrain the value of  $K_{Na}$  using an iterative approach to determine simultaneously the best-fitting stability constant values for Na and the adsorbing metal of interest.

In this approach, we fix a value for  $K_{Na}$ , and use the data to solve for a value for  $K_M$ . We systematically vary the fixed value for  $K_{Na}$  over a wide range of possible values, determining the value that yields the best overall fit to the data. The fixed value of  $\log K_{Na}$  was initially varied between 0 and 10, in increments of 1. For both the Li and Rb data, the model best fits the data when the  $\log K_{Na}$  value was fixed at 2. To more precisely determine the  $K_{Na}$  value, the value of  $\log K_{Na}$  was then varied between 1.0 and 3.0 in increments of 0.1 to determine the overall best fit for each metal.

We used the computer program FITEQL 2.0 (Westall 1982) to solve for the stability constants for the metal-bacterial surface complexes. This program accounts for the aqueous speciation of each metal, and all metal-surface complexes. Li, Rb, and Na are present almost exclusively as free monovalent cations in solution under our experimental conditions. We include aqueous cation hydrolysis reactions, using the constants reported by Baes and Mesmer (1976). The relative goodness of fit of each model is determined by comparing the overall variance parameter,  $V(Y)$ , calculated by FITEQL.

### Modeling of Monovalent Cation Adsorption to *B. subtilis*

Little adsorption of Li or Rb was observed at pH 3, and significant adsorption was observed in the pH 5, 7, and 9 experiments. Thus, we conclude that Site 1 (with a pKa value of 3.3) on the bacterial surface does not significantly contribute to the overall adsorption of monovalent cations. Adsorption of both Li and Rb increases significantly from pH 3 to pH 5, and we ascribe this increase to Li and Rb binding directly onto Site 2 (the site with a pKa value of 4.8). Thus, we determine the binding constants for the bacterial surface complexes that are formed by the binding of the monovalent cations onto Site 2, using the pH 5 data only and assuming that the adsorption under these pH conditions involves binding onto Site 2 only. This approach is reasonable because at pH 5 more than 98% of the Site 3 (with a pKa value of 6.8) functional groups are protonated and, therefore, are unlikely to contribute significantly to Li, Rb, or Na binding.

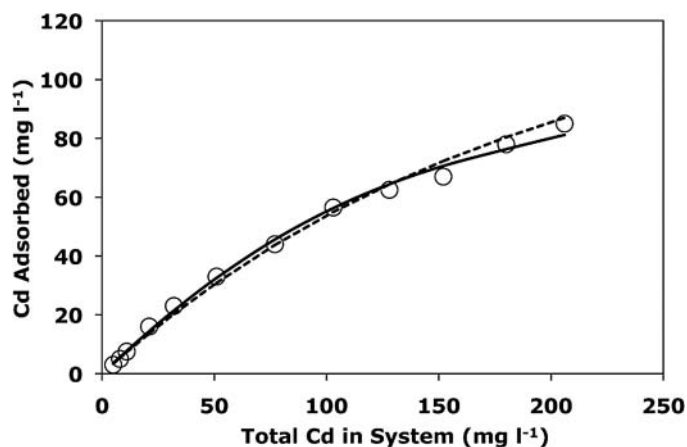


FIG. 4. Cd adsorption to  $10 \text{ g l}^{-1}$  *B. subtilis* cells in  $0.1 \text{ M NaClO}_4$  electrolyte at  $\text{pH } 5.9 \pm 0.2$ . Nonelectrostatic adsorption models with and without Na-Site 2 complexation included (both of which plot as the solid curve), and a diffuse layer adsorption model (dashed curve) yield similar good fits to the observed adsorption behavior. Data are from Mishra et al. (2008).

The best-fitting models to the pH 5 data for  $\text{Li}^+$  and  $\text{Rb}^+$  adsorption are shown as solid curves in Figures 1B and 2B, respectively. We calculate a  $\log K_{Li}$  value of 2.0, and a  $\log K_{Na}$  value of 2.3 using the pH 5  $\text{Li}^+$  adsorption data, and a  $\log K_{Rb}$  value of 1.9 and a  $\log K_{Na}$  value of 1.5 using the pH 5  $\text{Rb}^+$  adsorption data. To constrain the error of the  $\log K_{Rb}$  and  $\log K_{Li}$  values, we fixed the  $\log K_{Na}$  values in each model, and systematically varied the  $\log K_{Rb}$  and  $\log K_{Li}$  values in increments of  $\pm 0.1$  log units, calculating the extent of adsorption that would be predicted in each case. A variation of  $\pm 0.2$  log units in the Rb and Li  $\log K$  values (plotted as dashed curves in Figures 3 and 4, respectively) is sufficient to describe the variation in the data.

In order to test whether the monovalent cations adsorb to Sites 3 or 4 under our experimental conditions, we used the calculated  $K_{Na}$ ,  $K_{Li}$ , and  $K_{Rb}$  stability constants for Site 2 to predict the extent of Li or Rb adsorption that would occur at pH 7 and 9, assuming that only cation-Site 2 binding occurs for each metal. The results of this calculation for pH 7 and 9 appear in Figures 1A and 2A as grey and dashed curves, respectively. Li and Rb adsorption is predicted to increase somewhat from pH 5 to 7 and to remain essentially unchanged between pH 7 and 9 (Figures 1A, 2A). The predicted increase from pH 5 to 7 arises due to the higher concentration of deprotonated Site 2 sites at pH 7 relative to pH 5. From pH 7 to 9, there is little change in the concentration of deprotonated Site 2 sites, so the extent of cation binding onto Site 2 is predicted to remain constant for both Li and Rb.

The predicted increase in the extent of Rb adsorption from pH 5 to 7 is larger than that predicted over the same pH interval for Li adsorption because  $K_{Na}$  in the Li model is larger than  $K_{Li}$ , so as sites deprotonate going from pH 5 to 7, Na outcompetes Li for the available sites. The opposite trend occurs in the Rb model, where  $K_{Na}$  is smaller than  $K_{Rb}$  so Rb can better

compete with Na than does Li under the same circumstances. The observed extents of Li and Rb adsorption agree within experimental uncertainty with the predicted adsorption behaviors for the pH 7 and 9 conditions, suggesting that there is no significant interaction between the monovalent cations and Sites 3 or 4. Therefore, the only stability constants that we can determine from our data are those for the monovalent cations bound to Site 2.

The similarities in the log  $K$  values calculated for Li, Rb, and Na, and the relatively large uncertainties associated with them lead us to propose that reasonable estimates of the adsorption behavior of monovalent cations can be obtained by using a single averaged value for the stability constant for all monovalent cation-bacterial surface complexes. The average log  $K$  value, and associated  $\pm 1\sigma$  uncertainty for monovalent metal adsorption onto Site 2 of *B. subtilis* is  $1.9 \pm 0.3$ .

The first round of modeling, that yielded an average monovalent log  $K$  value of 1.9, used pKa and site concentration values directly from Fein et al. (2005). However, Fein et al. (2005) conducted potentiometric titrations of *B. subtilis* cells in the presence of a 0.1 M NaClO<sub>4</sub> matrix, but did not account for Na<sup>+</sup> competition with H<sup>+</sup> onto the cell wall sites.

Therefore, the protonation constants and site concentrations calculated by Fein et al. (2005) for cell wall functional groups must be adjusted to account for Na<sup>+</sup>-bacterial surface complexation. To accomplish this, we re-modeled data from a potentiometric titration of *Bacillus subtilis* cells from Fein et al. (2005), explicitly accounting for Na<sup>+</sup> complexation to the cell wall functional groups. In the initial model, we used the average monovalent  $K$  value of 1.9 from our first monovalent cation adsorption modeling as an initial estimate of the binding constant, even though this initial value was derived with the original pKa and site concentration values from Fein et al. (2005).

The best-fit new NEM of the potentiometric titration data involves 4 discrete sites on the bacterial cell wall. We used these newly calculated pKa and site concentration values, then, to recalculate an average monovalent  $K$  value from our Rb and Li adsorption data, following the same procedure as we did during the first modeling process. This iterative process was repeated until the pKa and monovalent  $K$  values changed less than 0.01 log units between iterations. The final pKa values and site concentrations of this model, and the corresponding values from a model of the potentiometric titration data which does not consider Na<sup>+</sup> complexation onto the cell wall functional groups, are listed in Table 1.

The calculated bacterial site concentrations are not significantly different between the two models. However, the model that includes Na<sup>+</sup> surface complexes yields pKa values that are approximately 0.7 log units lower than the model without Na<sup>+</sup> reactions. Additionally, the best-fit average monovalent log  $K$  value decreased from an initial value of  $1.9 \pm 0.3$  to a value of  $1.8 \pm 0.3$  as a result of this iterative modeling process.

The Li- and Rb-Site 2 stability constants are small relative to those of divalent and trivalent metals, consistent with our

observations of less extensive monovalent metal adsorption compared with that of higher charged cations. For example, using the same modeling approach applied here and the same reaction stoichiometries, Gorman-Lewis et al. (2005) report a log stability constant value of  $6.2 \pm 0.3$  for the binding of the uranyl cation (UO<sub>2</sub><sup>2+</sup>) to Site 2 of *B. subtilis*.

Similarly, Borrok et al. (2007) calculate Site 2 log stability constant values of 3.3 for Ni<sup>2+</sup> and 4.7 for Pb<sup>2+</sup>. Although these constants are large relative to those we calculate for monovalent cations in this study, monovalent cations are often present in natural systems and in laboratory experiments at concentrations that are orders of magnitude greater than those of the higher-charged cations of interest. Thus, monovalent cations may be able to compete effectively for adsorption onto bacterial surface functional groups in these experiments.

### Monovalent Cation Competition with Cd

Most experiments that have measured metal adsorption onto bacteria have been conducted using a monovalent electrolyte that is present at concentrations up to several orders of magnitude greater than that of the adsorbing metal of interest. Under these conditions, monovalent cations can compete effectively for surface sites. If metal adsorption in these studies is modeled using a nonelectrostatic approach and if the competition by monovalent cations is not accounted for in the thermodynamic calculations, then the calculated stability constants for the metal-bacterial surface complexes would need to be corrected.

We determine the magnitude of this correction for Cd-bacterial surface complexes, using Cd-*B. subtilis* adsorption data from pH-dependent adsorption experiments reported in this study (Figure 3A) and from isotherm adsorption data reported in Mishra et al. (2010) as examples. The data of Mishra et al. (2010), shown in Figure 4, were selected because they are isotherm experiments conducted as a function of Cd concentration at pH 5.9, so all of the Cd adsorption in these experiments can be attributed to Cd-Site 2 binding.

The experiments in Mishra et al. (2010) were conducted with 10 g l<sup>-1</sup> bacteria suspended in a 0.1 M NaClO<sub>4</sub> electrolyte at a fixed pH of  $5.9 \pm 0.2$ . Initial Cd solution concentrations in the experiments varied between 5 and 205 mg l<sup>-1</sup>. We use the same modeling approach employed by Mishra et al. (2010), but account for Na<sup>+</sup> binding to Site 2 in order to determine the magnitude of change in the calculated Cd stability constant for this site. The models that include Na<sup>+</sup> binding onto Site 2, also use the pKa and site concentrations that were calculated from models that include Na<sup>+</sup>-bacterial cell wall binding.

The models with and without Na<sup>+</sup>-Site 2 binding provide identical fits to the Cd adsorption data (Figure 4), but the stability constant calculated for the Cd-Site 2 surface complex increases significantly when the Na<sup>+</sup> competition reaction is considered. Without considering direct competition of Na<sup>+</sup> with Cd<sup>2+</sup>, and using the unadjusted Site 2 pKa value from Fein et al. (2005), the calculated best-fitting log stability constant value for the

Cd-Site 2 complex is 3.3. Including the Na-Site 2 complexation reaction, and using adjusted Site 2 pKa value from this study, yields a calculated best-fitting Cd-Site 2 log stability constant value of 4.2.

The NEM that we invoke is not a unique modeling approach to account for the Cd adsorption behavior in Figure 4. For example, these data can be fit equally well using an electrostatic diffuse layer model (DLM) and ignoring direct Na<sup>+</sup> binding to bacterial cell wall sites. In this approach, for consistency, we used FITEQL to re-model the *B. subtilis* potentiometric titration data using a 3-site DLM, and the results are tabulated in Table 1. The observed adsorption behavior can be described by invoking Cd complexation to Site 1 (pKa = 1.7). Figure 4 depicts the two NEM model fits (with and without Na<sup>+</sup> complexation; overlying solid lines) and the DLM fit (dashed line) of the Cd adsorption data. Both NEM and DLM models give excellent fits to the experimental data, however the NEM approach may be a more realistic and simple method to apply to geologic systems.

We model pH-dependent adsorption data between pH 2 and 5.5 (Figure 3A), using both NEM models (with and without Na<sup>+</sup> complexation). The calculated log stability constant value for the Cd-Site 2 complex is 4.0 without Na<sup>+</sup> competition considered (dashed curve). It was necessary to invoke Sites 2 and 3 (pKa values of 4.0 and 6.5 respectively) when using the NEM that includes Na<sup>+</sup> competition to fit these Cd adsorption data. In this exercise, we assume that the average monovalent binding constant values for Sites 2 and 3 are the same. The calculated best-fit Cd-Site 2 stability constant value is 3.8 and the Cd-Site 3 constant is 5.2 (solid curve). Notably, the model that includes the Na<sup>+</sup> competition reactions fits the data better than the model without this reaction. Additionally, the magnitude of the correction should be less for cations such as UO<sub>2</sub><sup>+2</sup> that display a higher affinity for the bacterial sites than does Cd<sup>+2</sup>.

The inclusion of Na<sup>+</sup> competition in bacterial cell wall speciation models significantly affects the calculated speciation of the cell wall functional groups. The differences in the speciation of Site 2 in models with and without the Na-Site 2 reaction are depicted in Figures 3B and 3C, respectively. In models that consider Na-Site 2 complexation, the Na-Site 2 complex represents the dominant surface species as the protonated site deprotonates with increasing pH. In addition, the stability of the Na-Site 2 complex is such that deprotonation occurs at lower pH than would be predicted from the model that does not consider Na-Site 2 complexation. Under the conditions of these calculations, when Na-Site 2 complexation is included, the model predicts that half of the Site 2 sites are protonated at approximately pH 3.1, whereas in models that neglect the Na-Site 2 complexation, this point occurs at pH 4.7. This same shift in speciation of the protonated site would occur if we modeled the reactions using electrostatic surface models.

The Na-Site 2 complexes represent the equivalent of Na<sup>+</sup> counterions that would be predicted to accumulate in the diffuse layer of electrostatic models, with the only difference being the location of the Na<sup>+</sup> cations relative to the cell wall functional

group sites. Therefore, for metabolically inactive *B. subtilis* cells, the site-specific Na-binding and electrostatic modeling approaches can successfully account for both multivalent cation adsorption caused by changes in ionic strength as well as the speciation of the surface induced by shifts in ionic strength. Metabolizing cells can generate a proton gradient near the cell wall, influencing its adsorption of metals (Urrutia Mera et al. 1992; Johnson et al. 2007). Further studies are needed to quantify this effect for monovalent metals.

## CONCLUSIONS

Our results demonstrate that monovalent cations adsorb to bacterial cell walls under some conditions, and that the adsorption can be modeled with site-specific adsorption reactions. With this approach, the ionic strength effect on metal adsorption onto bacteria can be modeled as a competition for available binding sites between the metal of interest and the monovalent cations of the background electrolyte. The stability constant values for Li-, Rb-, and Na-bacterial surface complexes are reasonably close to each other, and reasonable estimates of monovalent adsorption behavior can be achieved by assuming a universal stability constant for all monovalent-bacterial surface complexes.

Although monovalent cations adsorb much more weakly than do divalent and trivalent cations, in systems where the concentration of monovalent cations is much higher than that of the higher-charged metals that are present, the monovalent cations can effectively compete with other cations for available sites and diminish the extent of adsorption of those other cations. The approach of accounting for the ionic strength effect on adsorption by modeling it as competition for specific binding sites yields adsorption models that are easier to apply to complex geologic systems.

## REFERENCES

- Baes CF Jr., Mesmer RE. 1976. *The Hydrolysis of Cations*. Wiley: New York. 512 p.
- Beveridge TJ, Murray RGE. 1976. Uptake and retention of metals by cell walls of *Bacillus subtilis*. *J Bacteriol* 127:1502–1518.
- Beveridge TJ. 1989. Role of cellular design in bacterial metal accumulation and mineralization. *Annu Rev Microbiol* 43:147–171.
- Bjerrum N. 1926. The dilution heat of an ionic solution in the theory of Debye and Hueckel. Along with an article on the theory of heat effects in a dielectricum. *Z Phys Chem.-Stoch Ve* 119:145–160.
- Borrok DM, Turner BF, Fein JB. 2005. A universal surface complexation framework for modeling proton binding onto bacterial surfaces in geologic settings. *Am J Sci* 308:826–853.
- Borrok DM, Aumend K, Fein JB. 2007. Significance of ternary bacteria-metal-natural organic matter complexes determined through experimentation and chemical equilibrium modeling. *Chem Geol* 238:44–62.
- Covelo EF, Vega FA, Andrade ML. 2007. Competitive sorption and desorption of heavy metals by individual soil components. *J Hazard Mater* 140:308–315.
- Cox JS, Smith DS, Warren LA, Ferris FG. 1999. Characterizing heterogeneous bacterial surface functional groups using discrete affinity spectra for proton binding. *Environ Sci Technol* 33:4514–4521.

- Davis JA, James RO, Leckie JO. 1978. Surface ionization and complexation at the water/oxide interface. I. Computation of electrical double layer properties in simple electrolytes. *J Coll Interface Sci* 63:480–499.
- Davis JA, Kent DB. 1990. Surface complexation modeling in aqueous geochemistry. In: Hochella MF and White AF, editors. *Reviews in Mineralogy*, v. 23, Mineral-Water Interface Geochemistry. Mineralogical Society of America, Washington, DC. P 177–260.
- Davis JA, Coston JA, Kent DB, Fuller CC. 1998. Application of the surface complexation concept to complex mineral assemblages. *Environ Sci Technol* 32:2820–2828.
- Daughney CJ, Fein JB. 1998. The effect of ionic strength on the adsorption of  $H^+$ ,  $Cd^{2+}$ ,  $Pb^{2+}$ , and  $Cu^{2+}$  by *Bacillus subtilis* and *Bacillus licheniformis*: A surface complexation model. *J Coll Interf Sci* 198:53–77.
- Fein JB, Daughney CJ, Yee N, Davis TA. 1997. A chemical equilibrium model for metal adsorption onto bacterial surfaces. *Geochim Cosmochim Acta* 61:3319–3328.
- Fein JB, Boily J-F, Yee N, Gorman-Lewis D, Turner BF. 2005. Potentiometric titrations of *Bacillus subtilis* cells to low pH and a comparison of modeling approaches. *Geochim Cosmochim Acta* 69:1123–1132.
- Gorman-Lewis D, Elias PE, Fein JB. 2005. Adsorption of aqueous uranyl complexes onto *Bacillus subtilis* cells. *Environ Sci Technol* 39:4906–4912.
- Gu XY, Evans LJ. 2008. Surface complexation modelling of Cd(II), Cu(II), Ni(II), Pb(II) and Zn(II) adsorption onto kaolinite. *Geochim Cosmochim Acta* 72:267–276.
- Haas JR, Dichristina TJ, Wade R. 2001. Thermodynamics of U(VI) sorption onto *Shewanella putrefaciens*. *Chem Geol* 180:33–54.
- Johnson KJ, Ams DA, Wedel AN, Szymanowski JES, Weber DL, Schneegurt MA, Fein JB. 2007. The impact of metabolic state on Cd adsorption onto bacterial cells. *Geobiology* 5:211–218.
- Koretsky C. 2000. The significance of surface complexation reactions in hydrologic systems: A geochemist's perspective. *J Hydrol* 230:127–171.
- Ledin M, Pedersen K, Allard B. 1997. Effects of pH and ionic strength on the adsorption of Cs, Sr, Eu, Zn, Cd and Hg by *Pseudomonas putida*. *Water Air Soil Pollut* 93:367–381.
- Mishra B, Boyanov M, Bunker BA, Kelly SD, Kemner KM, Fein JB. 2010 (in press). High- and low-affinity binding sites for Cd on the bacterial cell walls of *Bacillus subtilis* and *Shewanella oneidensis*. *Geochim Cosmochim Acta*
- Ngwenya BT, Sutherland IW, Kennedy L. 2003. Comparison of the acid-base behaviour and metal adsorption characteristics of a gram-negative bacterium with other strains. *Appl Geochem* 18:527–538.
- Stumm W, Huang CP, Jenkins SR. 1970. Specific chemical interactions affecting the stability of dispersed systems. *Croatica Chemica Acta*, 24:223–244.
- Urrutia Mera M, Kemper M, Doyle R, Beveridge TJ. 1992. The membrane-induced proton motive force influences the metal-binding ability of *Bacillus subtilis* cell-walls. *Appl Environ Microbiol* 58:3837–3844.
- Westall JC. 1982. *FITEQL, A computer program for determination of chemical equilibrium constants from experimental data*. Version 2.0. Report 82-02, Dept. of Chemistry, Oregon State Univ., Corvallis, Oregon.
- Yee N, Fein J. 2001. Cd adsorption onto bacterial surfaces: A universal adsorption edge? *Geochim Cosmochim Acta* 65:2037–2042.